Assignment of paramagnetically shifted resonances in the ^{1}H NMR spectrum of horse ferricytochrome *c*

Yiqing Feng, Heinrich Roder, and S. Walter Englander
Department of Biochemistry and Biophysics, University of Pennsylvania, Philadelphia, Pennsylvania 19104-6059

ABSTRACT The proton resonances of the heme, the axial ligands, and other hyperfine-shifted resonances in the ^{1}H nuclear magnetic resonance spectrum of horse ferricytochrome *c* have been investigated by means of one- and two-dimensional nuclear Overhauser and magnetization transfer methods. Conditions for saturation transfer experiments in mixtures of ferro- and ferricytochrome *c* were optimized for the cross assignment of corresponding resonances in the two oxidation states. New resonance assignments were obtained for the methine protons of both thioether bridges, the β and γ meso protons, the propionate six heme substituent, the $N_\pi H$ of His-18, and the Tyr-67 OH. In addition, several recently reported assignments were confirmed. All of the resolved hyperfine-shifted resonances in the spectrum of ferricytochrome *c* are now identified. The Fermi contact shifts experienced by the heme and ligand protons are discussed.

INTRODUCTION

Since the early days of biological nuclear magnetic resonance (NMR), the *c*-type cytochromes have been among the most extensively studied proteins. Their small size and favorable solution properties make this class of proteins ideally suited for detailed ^{1}H NMR investigations. The presence of the paramagnetic heme in ferricytochrome *c* with its anisotropic *g*-tensor gives rise to large paramagnetic shifts for protons on or near the heme. Early work (1–3) focused on these resolved hyperfine-shifted resonances of the ferric form in order to obtain information about the electronic structure of the heme and its protein environment. Firm resonance assignments for heme and ligand protons were first obtained in the diamagnetic ferrous form of horse cytochrome *c* (4, 5), based on the nuclear Overhauser effect (NOE). By use of saturation transfer methods (3), some of these resonances were correlated with the corresponding resonances in the ferric form (4). Subsequent work resulted in extensive heme and side-chain resonance assignments in horse and tuna cytochrome *c* (6–10).

More recently, nearly complete assignments for the main chain proton resonances of horse cytochrome *c* in both oxidation states were obtained by two-dimensional NMR methods (11–14). The hyperfine-shifted resonances in the oxidized state are, however, not readily accessible to two-dimensional NMR study due to their extreme chemical shifts and short transverse relaxation times. At this stage, only a small number of protons remain unassigned, but these include some hyperfine-shifted protons resonating in crowded regions of the spectrum that are particularly difficult to find. In order to identify some of these elusive protons, we applied one- and two-dimensional NOE and magnetization transfer techniques in H_2O and D_2O solution. Experimental conditions were optimized for the observation of secondary nuclear Overhauser effects in the reduced form, following saturation transfer from the oxidized to the reduced form. Together with the recently reported assignments by Santos and Turner (10), the results provide a firm basis for further structural and functional studies of *c*-type cytochromes. For example, the contact-shifted heme and ligand protons represent sensitive probes of the electronic structure of the heme.

MATERIALS AND METHODS

Sample preparation

Horse heart cytochrome *c* (type VI; Sigma Chemical Co., St. Louis, MO) was used without further purification. Dithionite or ferricyanide was added in minimal amounts to prepare reduced or oxidized cytochrome *c*, respectively, and was removed by passing the solutions through Sephadex G-25 fine columns equilibrated with H_2O or D_2O solutions containing 150 mM sodium chloride and 100 mM sodium phosphate, pH or pD 5.7 (uncorrected reading at 25°C). Partially oxidized samples for magnetization transfer experiments were prepared by mixing appropriate amounts of fully reduced and fully oxidized cytochrome *c* solutions. The fraction of oxidized cytochrome *c* was 10–20% for one-dimensional saturation transfer experiments and 50%

Dr. Feng's present address is Department of Biochemistry, University of Illinois, Urbana, IL 61801.
Address correspondence to Heinrich Roder.

0006-3495/90/01/15/08 $2.00

for two-dimensional magnetization transfer experiments. The solutions were deoxygenated with argon gas in the NMR tube, and tight rubber stoppers were used to seal the tube. The ratio of reduced to oxidized cytochrome *c* was found to remain stable over a period of several days. Final cytochrome *c* concentrations were ~10 mM.

NMR spectroscopy

All ^{1}H NMR spectra were recorded at 20°C on a 500-MHz spectrometer (model AM-500; Bruker Instruments, Inc., Billerica, MA). One-dimensional saturation transfer and NOE spectra of samples in D_2O buffer were recorded by selective saturation of the resonance of interest for time periods of 50–500 ms before the 90° observe pulse. For each irradiation frequency, 80–1,600 transients were acquired, cycling through several on-resonance frequencies and one off-resonance frequency in blocks of 8 or 16 transients. Difference spectra were obtained by subtracting the free induction decays before Fourier transformation. For samples in 90% H_2O/10% D_2O buffer, the solvent signal was suppressed by replacing the observe pulse by a 1-1 (jump-and-return) pulse sequence (15). Two-dimensional NMR spectra were recorded as described previously (14, 16).

RESULTS AND DISCUSSION

Saturation transfer and secondary NOE

Cytochrome *c* in a mixture of oxidized and reduced forms is known to interconvert between the two oxidation states via electron transfer (3). Under suitable conditions, this redox exchange reaction is sufficiently rapid for saturation transfer experiments. When a resonance in one oxidation state is selectively saturated, the combination of cross relaxation and chemical exchange gives rise to three types of effects: (*a*) direct NOEs to neighboring protons in the same oxidation state; (*b*) transfer of saturation via electron exchange to the corresponding resonance in the other oxidation state; (*c*) secondary NOEs in the other oxidation state induced by the transferred magnetization (10). Since a molecule the size of cytochrome *c* gives rise to negative NOEs, all three effects have the same sign in a difference spectrum. If chemical exchange is fast compared with cross relaxation, the electron transfer effect dominates a difference spectrum at short irradiation times. The electron exchange rate in partially oxidized cytochrome *c* can be varied over a significant range by changing the ionic strength (17, 18). At the salt concentration chosen for this work (0.25 M), the redox exchange rate exceeds typical cross relaxation rates without causing significant exchange broadening.

Direct and secondary NOEs can in principle be distinguished by comparison with NOE difference spectra recorded on fully reduced and fully oxidized samples, or by measuring the NOE build-up curve, based on the fact that the initial rate of the secondary effect is zero. However, the former method cannot be applied in crowded regions of the spectrum, and the latter requires very accurate measurements at short irradiation times. As a practical approach to distinguishing the two effects, we chose to vary the equilibrium ratio of reduced and oxidized cytochrome *c*. Simple model calculations of the saturation transfer effect as a function of the redox equilibrium constant indicate that the transfer of saturation from the oxidized to the reduced form is most efficient when the fraction of the reduced form is ~90%. At such a biased ratio, secondary NOEs can be readily measured while NOEs in the oxidized form contribute little to the difference spectrum. This situation is in contrast to two-dimensional chemical exchange spectroscopy which is optimal at equal concentrations of the exchanging species.

The experimental data shown in Fig. 1 confirm the

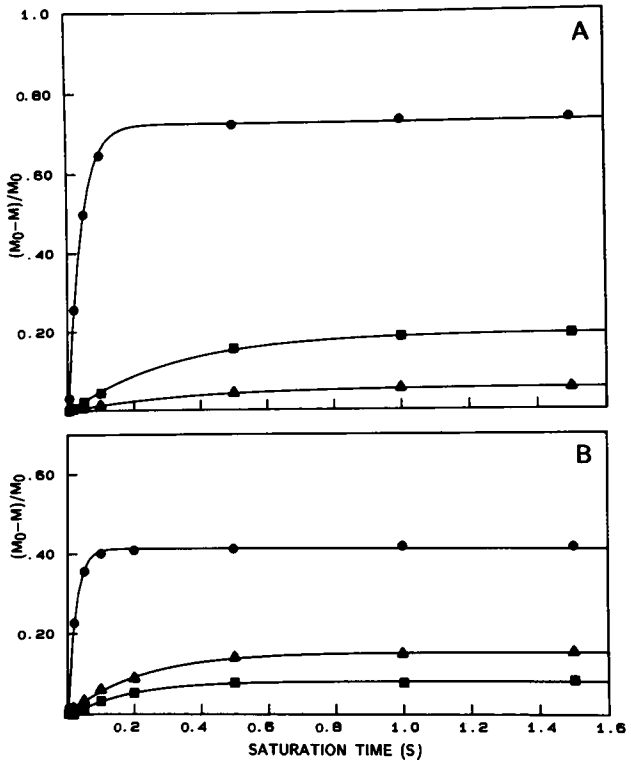

FIGURE 1 Time dependence of saturation transfer, direct NOE and secondary NOE in mixtures of reduced and oxidized cytochrome *c* for two samples containing 11% (*A*) and 48% (*B*) oxidized protein, respectively. In both cases, the heme ring-3 methyl resonance in the oxidized form was selectively saturated for variable time periods. The normalized intensity change, $(M_o - M)/M_o$, is plotted as a function of the saturation time for the ring-3 methyl resonance in the reduced form (●, saturation transfer), for the bridge-4 methyl resonance in the oxidized form (▲, direct NOE) and for the bridge-4 methyl resonance in the reduced form (■, secondary NOE). The curves represent least-squares exponential fits to the data.

calculations. When the fraction of reduced cytochrome *c* is increased from 52% (Fig. 1 *B*) to 89% (Fig. 1 *A*), the steady-state intensity of the electron transfer effect increases from ~40% to ~70%, and that of the secondary NOE increases from <10% to 20%, exceeding the intensity of the direct NOE effect by a factor of three. A similar pattern can be observed under pre–steady state conditions. The initial saturation transfer rate, which represents the sum of the longitudinal relaxation rate and the rate of oxidation (19), is about an order of magnitude faster than the cross-relaxation rate. Using an independent measurement of the T_1 relaxation time (unpublished results), we find a second-order electron transfer rate of ~100 $M^{-1}s^{-1}$, which is somewhat higher than the rate reported by Gupta et al. (17), probably due to differences in sample conditions.

When this work was initiated, only a limited number of assignments were known in oxidized cytochrome *c* while a much larger number of assignments were available for the reduced protein (11, 12, 20). Secondary NOEs proved to be valuable for the assignment of resonances in oxidized cytochrome *c* in situations where conventional saturation transfer experiments were inconclusive; when the corresponding resonance in the reduced form is poorly resolved, the ambiguity can often be resolved by considering the pattern of secondary NOEs to previously assigned resonances in the reduced form. Another advantage lies in the ability to observe cross-relaxation in the diamagnetic reduced form where NOEs are generally stronger than in the paramagnetic oxidized form. This situation is analogous to the transferred NOE method used for the structural analysis of ligand–protein complexes (21).

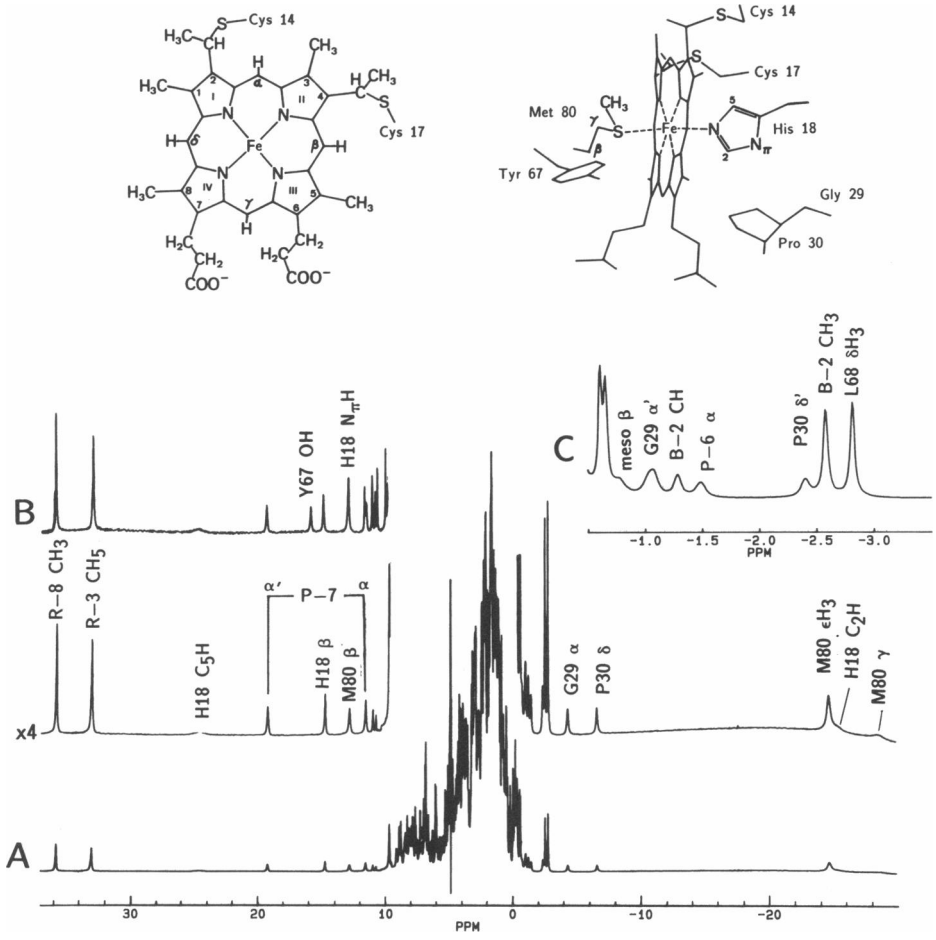

FIGURE 2 (*A*) ^{1}H NMR spectrum of horse ferricytochrome *c* in D_2O 100 mM phosphate, 150 mM NaCl, pD 5.7, recorded at 20°C. (*B*) Downfield region of a spectrum recorded under the same conditions on a sample in 90% H_2O/10% D_2O solutions, indicating several hyperfine-shifted resonances of exchangeable protons. (*C*) Expanded plot of the region between −0.5 ppm and −3.5 ppm in spectrum *A*. The abbreviations used for the heme substituents are R-, B-, and P- for the ring methyls, thioether bridges, and propionates, respectively. The structure of the heme and selected sidechains, drawn according to the x-ray coordinates (23), is shown on top.

Assignment of hyperfine-shifted resonances

The ^1H NMR spectrum of horse ferricytochrome *c* in D_2O at 20°C is shown in Fig. 2, along with an expanded trace of the low-field region recorded in H_2O. The notation used is indicated in a diagram of the heme and surrounding side chains. The chemical shifts for assigned hyperfine-shifted resonances are listed in Table 1, including previously reported assignments that were confirmed in this work.

The use of secondary NOEs as an assignment tool is illustrated in trace *A* of Fig. 3. Selective saturation of the resonance at 12.85 ppm in D_2O solution results in an exchange effect at −0.20 ppm, which coincides with the chemical shift of Met-80 $C_\beta H$ in the reduced form (22), and secondary NOEs to all other resonances associated with the Met-80 spin system of the reduced protein (2, 11, 22). The pair of lines at 12.85 ppm and −0.2 ppm in the oxidized and reduced form, respectively, are thus unambiguously assigned to one of the Met-80 $C_\beta H$, in agreement with the result of Santos and Turner (10). However, we were not able to confirm their assignment for the other β proton of Met-80 (3.0 ppm at 30°C). Irradiation at 12.85 ppm in fully oxidized cytochrome *c* results in a single NOE at 3.54 ppm. This shift coincides with the methyl group of Thr-78 (8, 14) which is within NOE distance of the Met-80 $C_\beta H_2$ (23). This leaves one of the Met-80 β protons still unassigned, possibly because it relaxes too fast to give rise to an observable NOE.

Comparing the spectra of oxidized cytochrome *c* recorded in H_2O and in D_2O (Fig. 2, *A* and *B*), it is apparent that a labile proton also resonates at 12.85 ppm. The two resonances are degenerate at 20°C, but are resolved at other temperatures; e.g., at 10°C the labile proton resonance appears at 13.04 ppm while the nonlabile one moves to 13.71 ppm. For the assignment of the labile proton we performed a saturation transfer experiment in H_2O solution using a 1-1 observation pulse for the suppression of the water signal (Fig. 3 *B*). The major difference compared with the corresponding experiment in D_2O (Fig. 3 *A*) is a prominent exchange peak at 9.65 ppm. The only exchangeable proton resonance at this position in the reduced spectrum that remains unassigned

TABLE 1 Resonance assignments for heme and ligand protons in horse cytochrome *c* at pH 5.7 and 20°C

Assignment		Oxidized	Reduced
Heme			
Meso-β		−0.78	9.60 (4)
Meso-γ		8.02	9.63 (4)
Ring-1	CH_3	6.8 (4)	3.52 (4)
Ring-3	CH_3	33.1 (4)	3.85 (4)
Ring-5	CH_3	9.7 (4)	3.61 (4)
Ring-8	CH_3	35.9 (4)	2.18 (4)
Bridge-2	CH	−1.28	5.23 (4)
	CH_3	−2.55 (4)	1.49 (4)
Bridge-4	CH	2.18	6.36 (4)
	CH_3	3.15 (4)	2.61 (4)
Propionate-6	$C_\alpha H$	−1.47	4.19
		1.76	
	$C_\beta H_2$	2.77	
		1.17	
Propionate-7	$C_\alpha H_2$	19.37 (9, 23)	3.64 (10)
		11.52 (9, 23)	4.17 (10)
	$C_\beta H_2$	1.62 (10)	
		−0.38 (10)	
His-18	$C_\beta H_2$	9.00 (9, 23)	0.79 (13)
		14.82 (9, 23)	1.08 (10, 13)
	C2H	−25.60 (10)	0.52 (6, 11)
	C5H	24.90 (10)	0.13 (6, 11)
	NπH	12.85	9.65 (12)
Met-80	$C_\beta H$	12.85 (10)	−0.20 (22)
	$C_\gamma H$	−28.5 (3)	−3.75 (2)
	$C_\epsilon H_3$	−24.7 (1)	−3.28 (2)
Tyr-67 OH		15.80	3.11

Chemical shifts (ppm) are referenced to TSP (3-trimethylsilyl-[2,2,3,3-^2H] propionic acid), in D_2O or 90% H_2O/10% D_2O with 0.1 M $NaPO_4$ and 0.15 M NaCl. References for previously assigned resonances are indicated in parentheses.

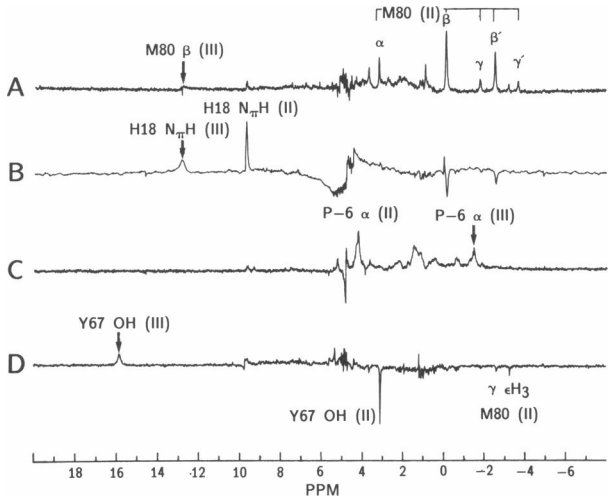

FIGURES 3 Saturation transfer difference spectra recorded on partially oxidized cytochrome *c* (same conditions as in Fig. 2). The following resonances (indicated by arrows) were irradiated: (*A*) Met-80 $C_\beta H$ (irradiation time 400 ms); (*B*) His-18 $N_\pi H$ (200 ms); (*C*) propionate-6 (P-6) $C_\alpha H$ (50 ms); (*D*) Tyr-67 OH (270 ms). Traces *B* and *D* were recorded in H_2O solution, using a (1,1) pulse sequence (reference 15) for solvent suppression which results in a phase inversion at the carrier frequency. All other spectra were recorded in D_2O solution without solvent suppression. Resonance assignments in the reduced form (II) and the oxidized form (III) are indicated for the major effects in the difference spectra (see Fig. 2 for nomenclature). Artifacts at the H_2O frequency were in some cases removed by digital manipulation of a few data points.

in the oxidized form is the ring $N_\pi H$ of His-18 (13). The labile proton resonance at 12.85 ppm is thus assigned to His-18 $N_\pi H$ in the ferric form.

The histidine ring NH is involved in a crystallographically defined hydrogen bond with the carbonyl oxygen of Pro-30 (24). This interaction appears to be important for positioning the axial histidine ligand and is expected to affect the exchange behavior of the ring proton. The His-18 $N_\pi H$ thus represents an interesting dynamic probe for investigating structural fluctuations in the vicinity of the histidine ligand.

Fig. 2 *B* exhibits a second unassigned resonance from an exchangeable proton in an extreme downfield position (15.80 ppm). Saturation of this line in a partially oxidized sample (Fig. 3 *D*) shows a clear chemical exchange effect at 3.10 ppm and secondary NOEs to the resolved Met-80 $C_\gamma H$ and $C_\epsilon H_3$ lines (−2.61 ppm and −3.28 ppm). Inspection of the crystal structure shows that the only exchangeable proton within a 6-Å radius of the Met-80 methyl is the OH of Tyr-67 (see Fig. 2). Hydroxyl protons are rarely observed due to their rapid exchange rate, but in this case the exchange rate is reduced by the fact that the hydroxyl proton is hydrogen bonded to the Met-80 sulfur (24). This assignment relies primarily on secondary NOEs in the reduced form, since the width of the Met-80 resonances in the paramagnetic state makes it difficult to observe NOEs directly in the oxidized form.

Previous assignments for the heme propionate-7 substituent in both oxidation states (9, 10, 25) were confirmed by a series of NOE and saturation transfer experiments. The other propionate sidechain, propionate-6, does not give rise to resolved resonances, and it was necessary to employ two-dimensional NMR methods. The cross section shown in Fig. 4 *A*, taken from a two-dimensional NOE Spectroscopy (NOESY) spectrum on ferricytochrome *c*, indicates that the proton resonating at −1.47 ppm is spatially close to the heme ring-5 methyl group. Inspection of the crystal structure (23, 24) reveals that propionate-6 is the only possible candidate. The other protons on the propionate-6 side chain were assigned on the basis of the relative NOE intensities (Fig. 4 *A*) and the coupling pattern in the two-dimensional J-correlated spectrum (Fig. 5). The C_α proton resonance at −1.47 ppm was shown by saturation transfer to be associated with a resonance at 4.19 ppm in the spectrum of the reduced protein (Fig. 3 *C*).

An earlier assignment for the thioether bridge-2 methyl group at −2.55 ppm in the ferric state (3, 4) was extended to the methine proton (−1.28 ppm) on the basis of the phase-sensitive double-quantum filtered COSY (DQF-COSY) spectrum shown in Fig. 4 and by a chemical exchange correlation (not shown) between −1.28 ppm and the known methine chemical shift in the reduced form (5.23 ppm). Since the bridge-4 CH is unresolved in

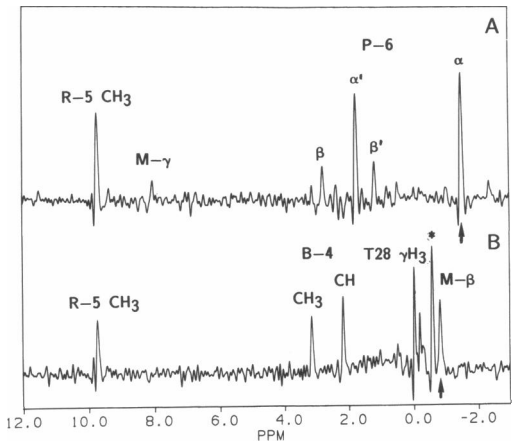

FIGURE 4 Cross sections of a NOESY spectrum of ferricytochrome *c* recorded in D_2O buffer, taken along the ω_2 axis at the frequencies of the propionate-6 $C_\alpha H$ (−1.47 ppm) (*A*) and the meso-β (M − β) proton (−0.78 ppm) (*B*). The diagonal peaks are indicated with arrows. The peak marked with an asterisk results from the partial overlap of meso-β with Ile-57 $C_\delta H_3$.

both oxidation states, its assignment in the oxidized form (2.18 ppm) relied on relayed exchange effects in a two-dimensional total correlation spectroscopy (TOCSY) experiment on partially oxidized cytochrome *c* (16). Fig.

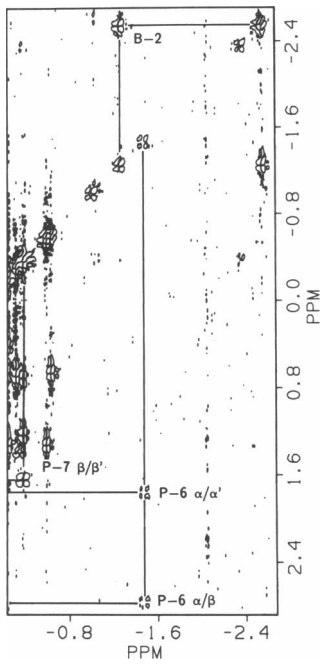

FIGURE 5 Expanded contour plot of a phase sensitive two-dimensional J-correlated spectrum (DQF-COSY) of ferricytochrome *c*. The heme bridge-2 CH-CH_3 cross peak (B-2) and partial spin systems for propionate-6 (P-6) and propionate-7 (P-7) are indicated.

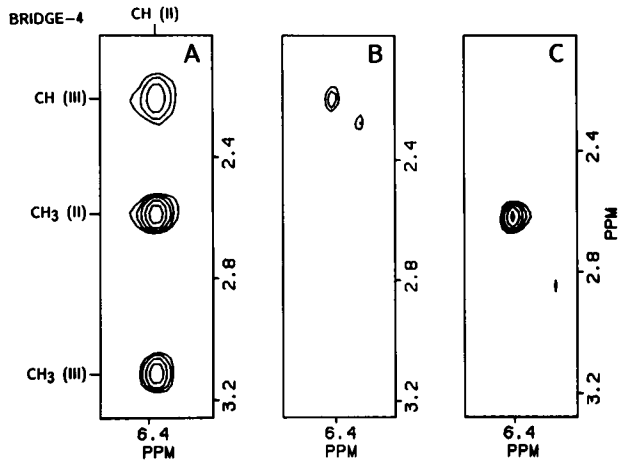

FIGURE 6 (*A*) Expanded section of a TOCSY spectrum of a partially oxidized cytochrome *c* sample containing cross peaks assigned to thioether bridge-4. Chemical exchange and J-coupling cross peaks are identified in panels *B* and *C*, which show expansions of the same spectral region for a chemical exchange spectrum (NOESY) recorded on a partially oxidized sample (*B*), and a TOCSY spectrum recorded on a fully reduced sample (*C*).

6 *A* shows an expanded region of the TOCSY spectrum containing three cross peaks associated with the bridge-4 methine resonance in the reduced state (6.36 ppm). The cross peak at 2.18 ppm is identified by the two-dimensional chemical exchange spectrum shown in Fig. 6 *B* as the exchange correlation between the methine resonances in the two oxidation states. The J-correlated spectrum shown in Fig. 6 *C* shows that the cross peak at 2.61 ppm is due to J-coupling between the methine and methyl protons in the reduced form. The third cross peak (ω_1 = 3.15 ppm) in the TOCSY spectrum is thus the result of relayed magnetization transfer from the methine resonance in the reduced form to the methyl resonance in the oxidized form.

The four heme meso protons have been individually assigned for reduced cytochrome *c* (4), but remain to be identified in the spectrum of oxidized cytochrome *c*. The assignment of the meso-β was straightforward, based on an unambiguous exchange correlation with the corresponding resonance in the reduced state (9.60 ppm) in the two-dimensional chemical exchange spectrum. This correlation was further confirmed by a TOCSY experiment on partially oxidized cytochrome *c* (c.f. Fig. 6), which exhibits a positive cross peak in the same position (note that cross-correlation effects give rise to negative TOCSY cross peaks). In the oxidized form, this resonance exhibits several strong NOEs to the heme protons adjacent to the meso-β (bridge-4 and ring-5) and to a nearby methyl group (Thr-28) as shown in Fig. 5 *B*. For the meso-γ resonance (9.63 ppm in the reduced form), only a rather weak redox exchange cross peak was found at 8.02 ppm, which was again confirmed by an unambiguous exchange effect in the TOCSY experiment. The meso-γ assignment is further supported by NOEs to propionate-6 (Fig. 5 *A*) and propionate-7 $C_\alpha H_2$ (not shown).

The C_2H and C_5H (IUPAC; C_4H in the old convention) of the axial His-18 ligand have only recently been correctly assigned (10) to two broad lines in extreme upfield and downfield positions, respectively (Fig. 2). This surprising result was confirmed by our work (Table 1), based on saturation transfer effects and secondary NOEs to the newly assigned His-18 $N_\pi H$ and to Pro-30 $C_\delta H_2$.

In addition to the heme and the axial ligands, large paramagnetic shifts are also observed for Gly-29 and Pro-30 which are in the immediate vicinity of the heme (Fig. 2). Our saturation transfer and NOE results on these resonances are fully consistent with the recent report of Santos and Turner (10).

Hyperfine shifts

The resonance assignments summarized in Table 1 provide a basis for further analysis of paramagnetic shift mechanisms. The observed chemical shift in ferricytochrome *c*, δ_{ox}, can be written as $\delta_{ox} = \delta_d + \delta_{pc} + \delta_c$, where δ_d is the diamagnetic contribution to chemical shift, δ_{pc} describes the pseudocontact shift due to dipolar interaction with the unpaired electron spin, and δ_c represents the scalar Fermi contact interaction. Assuming that the structure of oxidized cytochrome *c* is similar to that of the reduced protein, δ_d can be approximated by the measured shift in the reduced form, δ_{red} (13). The total hyperfine shift is then $\delta_{hf} = \delta_{ox} - \delta_{red}$. For the limit of short electronic spin lattice relaxation times, δ_{pc} is given by a well-known expression (26) which relates the dipolar shift to the principal *g*-tensor components and the nuclear coordinates. The contact term reflects the unpaired electron spin density at the site of a nucleus and is expected to be significant only for the protons of the heme and its ligands.

Contact shifts can provide valuable information on the electronic structure of the heme (27, 28), and have potential functional implications (4, 29). However, the analysis of contact shifts is complicated by the problem of separating the different chemical shift contributions. Williams et al. (30) analyzed the pseudocontact shifts in tuna ferricytochrome *c* using assigned methyl resonances (8) to calibrate the *g*-tensor components in solution. Recent calculations on horse cytochrome *c* (31), using a large set of assigned C_α proton resonances (14) for the refinement of the *g*-tensor, will be reported elsewhere (Feng, Y., H. Roder, and S. W. Englander, submitted for publication). For many heme and ligand protons the calculated pseudo-

contact shift makes a significant contribution to the total hyperfine shift. Due to the proximity of these protons to the heme iron, their pseudocontact shift is extremely sensitive to small changes in the proton coordinates and the *g*-tensor. In view of these uncertainties, only a qualitative discussion of contact shifts can be given at this stage.

The analysis of the ring methyl shifts in ferricytochrome *c* (2–4) and other heme proteins (reviewed in reference 32) has led to the conclusion that the distribution of the unpaired electron spin over the heme is strongly asymmetric. The large shift difference between the two meso protons assigned in this work (Table 1) is consistent with this asymmetry. The β and γ meso protons are shifted upfield from the diamagnetic resonance position by 10.4 ppm and 1.6 ppm, respectively. The meso-γ shift is similar to shifts reported for the meso protons in the cyanide complex of Fe(III) protoporphyrin IX (33). The contact shift estimated by subtraction of the calculated δ_{pc} has opposite sign for the two meso protons.

For the methine protons of both thioether bridges, the theoretical pseudocontact shift matches the experimental hyperfine shift (Table 1) within 1 ppm. This indicates that only a small amount of unpaired electron spin density is delocalized into the thioether bridges, which confirms earlier results on the thioether methyl groups (4). The dipolar shift calculation largely accounts for the hyperfine shift of the propionate-6 α proton, but the downfield shift of the propionate-7 α protons (Table 1) is dominated by contact interactions. This result is consistent with the shift pattern observed for the ring methyl protons (4): the contact contribution is small for the heme substituents of pyrrole III (ring-5 methyl and propionate-6), while the substituents of pyrrole IV (ring-8 methyl and propionate-7) experience large contact shifts. The large shift difference between the two geminal propionate-7 α protons (>7 ppm) is an illustration of the theoretically expected dependence of the contact shift on the orientation of the C-H bond relative to the heme plane (27).

Some of the earliest resonance assignments in ferricytochrome *c* were obtained for protons of the axial methionine ligand (1–3). The extreme upfield position of the $C_\epsilon H_3$ and $C_\gamma H$ (Fig. 2) is largely due to contact shifts. These effects are comparable in magnitude to those experienced by the ring methyls, but opposite in sign. By contrast, the hyperfine shift of the Met-80 $C_\beta H$ resonance, 13 ppm downfield from its diamagnetic position (Table 1), is well predicted by the pseudocontact-shift calculation. The chemical shift pattern for the other axial ligand, the His-18 imidazole ring, with hyperfine shifts ($\delta_{ox} - \delta_{red}$) of −26 ppm, 25 ppm, and 3 ppm for the C_2H, C_5H, and $N_\pi H$, respectively, appears at first rather puzzling. However, after subtraction of the calculated dipolar shift (Feng, Y., H. Roder, and S. W. Englander, submitted for publication), it appears that all the His-18 ring protons experience a negative (upfield) contact contribution. Among the three ring protons, the C_2H exhibits the largest contact contribution, which can be rationalized by the fact that the N_π—C_2 bond has more double bond character than the N_π—C_5 bond. For the His-18 β protons, a relatively small positive contact shift is estimated. Both axial ligands thus show a similar pattern of contact shifts. The two protons adjacent to the ligand atoms experience large negative contact shifts, while the effect is much smaller for protons separated by four or more bonds from the iron.

This work was supported by National Institutes of Health research grants GM-31847 (Dr. Englander) and GM-35926 (Dr. Roder).

Received for publication 23 March 1989 and in final form 24 July 1989

REFERENCES

1. Wüthrich, K. 1969. High-resolution proton nuclear magnetic resonance spectroscopy of cytochrome c. *Proc. Natl. Acad. Sci. USA.* 63:1071–1078.
2. McDonald, C. C., W. D. Phillips, and S. N. Vinogradov. 1969. Proton magnetic resonance evidence for methionine-iron coordination in mammalian-type ferrocytochrome c. *Biochem. Biophys. Res. Commun.* 36:442–449.
3. Redfield, A. G., and R. J. Gupta. 1971. Pulsed NMR study of the structure of cytochrome c. *Cold Spring Harbor Symp. Quant. Biol.* 36:405–411.
4. Keller, R. M., and K. Wüthrich. 1978. Assignment of the heme c resonances in the 360 MHz ^{1}H NMR spectrum of cytochrome c. *Biochim. Biophys. Acta.* 533:195–208.
5. Gordon, S. L., and K. Wüthrich. 1978. Transient proton-proton Overhauser effects in horse ferrocytochrome c. *J. Am. Chem. Soc.* 100:7094–7096.
6. Moore, G. R., and R. J. P. Williams. 1980. Nuclear magnetic resonance studies of eucaryotic cytochrome c. Assignment of resonances of aromatic amino acids. *Eur. J. Biochem.* 103:493–502.
7. Moore, G. R., and R. J. P. Williams. 1980. Nuclear magnetic resonance studies of eucaryotic cytochrome c. Assignment of resonances of aliphatic amino acids. *Eur. J. Biochem.* 103:503–512.
8. Williams, G., G. R. Moore, R. Porteous, M. N. Robinson, N. Soffe, and R. J. P. Williams. 1985. Solution structure of mitochondrial cytochrome c. I. ^{1}H nuclear magnetic resonance of ferricytochrome c. *J. Mol. Biol.* 183:409–428.
9. Satterlee, J. D., and S. Moench. 1987. Proton hyperfine resonance assignments using the nuclear Overhauser effect for ferric forms of horse and tuna cytochrome c. *Biophys. J.* 52:101–107.
10. Santos, H., and D. L. Turner. 1987. Proton NMR studies of horse ferricytochrome c. *FEBS (Fed. Eur. Biochem. Soc.) Letts.* 226:179–185.
11. Wand, A. J., and S. W. Englander. 1985. Two-dimensional ^{1}H NMR studies of cytochrome c. *Biochemistry.* 24:5290–5294.
12. Wand, A. J., and S. W. Englander. 1986. Two-dimensional ^{1}H

NMR studies of cytochrome c: assignment of the N-terminal helix. *Biochemistry*. 25:1100–1106.

13. Wand, A. J., D. L. Di Stefano, Y. Feng, H. Roder, and S. W. Englander. 1989. Proton resonance assignments of horse ferrocytochrome c. *Biochemistry*. 28:189–194.
14. Feng, Y., H. Roder, S. W. Englander, A. J. Wand, and D. L. Di Stefano. 1989. Proton resonance assignments of horse ferricytochrome c. *Biochemistry*. 28:195–203.
15. Plateau, P., and M. Gueron. 1982. Exchangeable proton NMR without base-line distortion, using new strong-pulse sequences. *J. Am. Chem. Soc.* 104:7310–7311.
16. Feng, Y., and H. Roder. 1988. Relayed magnetization transfer by isotropic mixing in exchanging systems. *J. Magn. Reson.* 78:597–602.
17. Gupta, R. K., S. H. Koenig, and A. G. Redfield. 1972. On the electron transfer between cytochrome c molecules as observed by nuclear magnetic resonance. *J. Magn. Reson.* 7:66–73.
18. Boyd, J., G. R. Moore, and G. Williams. 1984. Correlation of protein chemical shifts in proteins using two-dimensional exchange correlated spectroscopy. *J. Magn. Reson.* 58:511–516.
19. Forsen, S., and R. A. Hoffman. 1963. Study of moderately rapid chemical exchange reactions by means of nuclear magnetic double resonance. *J. Chem. Phys.* 39:2892.
20. Moore, G. R., M. N. Robinson, G. Williams, and R. J. P. Williams. 1985. Solution structure of mitochondrial cytochrome c. II. ^{1}H nuclear magnetic resonance of ferrocytochrome c. *J. Mol. Biol.* 183:429–446.
21. Clore, G. M., and A. M. Gronenborn. 1983. Theory of the time dependent transferred nuclear Overhauser effect: applications to structural analysis of ligand-protein complexes in solution. *J. Magn. Reson.* 53:423–442.
22. Keller, R. M., and K. Wüthrich. 1981. ^{1}H-NMR studies of structural homologies between the heme environments in horse cytochrome c and in cytochrome c-552 from *Euglena gracilis*. *Biochim. Biophys. Acta*. 668:307–320.
23. Takano, T., and R. E. Dickerson. 1981. Conformation change of cytochrome c. II. Ferricytochrome c structure refined at 1.5 Å resolution and comparison with the ferrocytochrome structure. *J. Mol. Biol.* 153:95–115.
24. Takano, T., and R. E. Dickerson. 1981. Conformation change of cytochrome c. I. Ferrocytochrome c structure refined at 1.5 Å resolution. *J. Mol. Biol.* 153:79–94.
25. Moore, G. R., and G. Williams. 1984. Assignment of ^{1}H-NMR resonances of the heme and axial histidine ligand of mitochondrial cytochrome c. *Biochim. Biophys. Acta*. 788:147–150.
26. Kurland, R. J., and B. R. McGarvey. 1970. Isotropic shifts in transition metal complexes: the calculation of the Fermi contact and pseudocontact terms. *J. Magn. Reson.* 2:286–301.
27. Shulman, R. G., S. H. Glarum, and M. Karplus. 1971. Electronic structure of cyanide complexes of hemes and heme proteins. *J. Mol. Biol.* 57:93–115.
28. Wüthrich, K. 1976. NMR in biological research: peptides and proteins. Elsevier/North-Holland, Amsterdam/New York.
29. Senn, H., R. M. Keller, and K. Wüthrich. 1980. Different chirality of the axial methionine in homologous cytochromes c determined by ^{1}H NMR and CD spectroscopy. *Biochem. Biophys. Res. Commun.* 92:1362–1369.
30. Williams, G., N. J. Clayden, G. R. Moore, and R. J. P. Williams. 1985. Comparison of the solution and crystal structures of mitochondrial cytochrome c. *J. Mol. Biol.* 183:447–460.
31. Feng, Y. 1989. Two-dimensional NMR study of the structure of ferricytochrome c. Ph.D. thesis. University of Pennsylvania, Philadelphia, PA.
32. Satterlee, J. D. 1986. NMR spectroscopy of paramagnetic heme proteins. *Annu. Rep. NMR Spectrosc.* 17:79–178.
33. Wüthrich, K., R. G. Shulman, B. J. Wyluda, and W. S. Caughey. 1969. Proton magnetic resonance studies of prophyrin iron (III) cyanides. *Proc. Natl. Acad. Sci. USA*. 62:636–649.